Impedimetric DNA Detection–Steps Forward to Sensorial Application

ARTICLE *in* ANALYTICAL CHEMISTRY · JULY 2014

Impact Factor: 5.64 · DOI: 10.1021/ac501800q · Source: PubMed

4 AUTHORS, INCLUDING:

Marc Riedel
Technische Hochschule Wildau
6 PUBLICATIONS **31** CITATIONS
SEE PROFILE

Julia Kartchemnik
Technische Hochschule Wildau
1 PUBLICATION **8** CITATIONS
SEE PROFILE

Fred Lisdat
Technische Hochschule Wildau
172 PUBLICATIONS **3,726** CITATIONS
SEE PROFILE

analytical chemistry

Article

pubs.acs.org/ac

Impedimetric DNA Detection—Steps Forward to Sensorial Application

Marc Riedel,[†] Julia Kartchemnik,[†] Michael J. Schöning,[‡] and Fred Lisdat*[,†]

[†]Biosystems Technology, Institute of Applied Life Sciences, Technical University of Applied Sciences Wildau, Hochschulring 1, 15745 Wildau, Germany

[‡]Institute of Nano- and Biotechnologies, University of Applied Sciences Aachen, Heinrich-Mußmann-Strasse 1, 52428 Jülich, Germany

ABSTRACT: This study describes a label-free impedimetric sensor based on short ssDNA recognition elements for the detection of hybridization events. We concentrate on the elucidation of the influence of target length and recognition sequence position on the sensorial performance. The impedimetric measurements are performed in the presence of the redox system ferri-/ferrocyanide and show an increase in charge transfer resistance upon hybridization of ssDNA to the sensor surface. Investigations on the impedimetric signal stability demonstrate a clear influence of the buffers used during the sensor preparation and the choice of the passivating mercaptoalcanol compound. A stable sensor system has been developed, enabling a reproducible detection of 25mer target DNA in the low nanomolar range. After hybridization, a sensor regeneration can be reached with deionized water by adjustment of effective convection conditions, ensuring a sensor reusability. By investigations of longer targets with overhangs exposed to the solution, we can demonstrate applicability of the impedimetric detection for longer ssDNA. However, a decreasing charge transfer resistance change (ΔR_{ct}) is found by extending the overhang. As a strategy to increase the impedance change for longer target strands, the position of the recognition sequence can be designed in a way that a small overhang is exposed to the electrode surface. This is found to result in an increase in the relative R_{ct} change. These results suggest that DNA and consequently negative charge near the electrode possess a larger impact on the impedimetric signal than DNA further away.

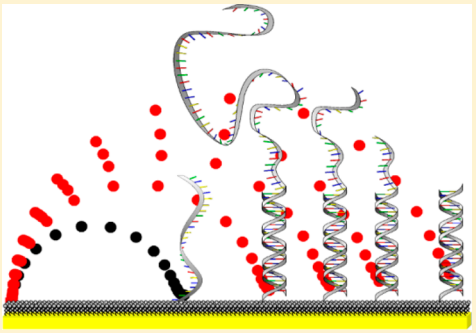

Bioanalysis in the fields of medicine, food industry, and environmental control strives for easy and fast nucleic acid detection devices with a high accuracy and low costs. Several applications in research and analytical laboratories have already been developed for the recognition of genetically originated diseases, the identification of pathogenic species, the detection of contaminations in food, or forensic studies. In addition to already applied detection methods, as e.g. PCR, also DNA biosensors (or genosensors) have been followed with growing interest during the past decade.[1−6] The operation principle of DNA biosensors is commonly based on a specific hybridization event between an immobilized single-stranded DNA (probe ssDNA) and complementary target ssDNA in a sample solution, which triggers the transduction to an analytical signal. Here, various transducers such as piezoelectric,[7,8] optical,[9−11] or electrochemical systems[1,2,12−16] have been used for analysis of the hybridization-induced change of the surface properties. Especially, electrochemical biosensors are promising for utilization in point-of-care diagnostics due to the potential for simple, cheap, and portable application.[4] Furthermore, electrochemical detectors benefit from developments in microfluidics, microsystems technology or nanotechnology, which enable miniaturization processes and offer the possibility of parallel high throughput detection. Several approaches have been demonstrated to detect hybridization reactions by electrochemical methods. In most cases, a redox molecule is required for the detection process of the hybridization event. Often, a redox or enzymatic label needs to be coupled covalently to the target molecule, which causes a high sensitivity but also a more expensive and time-consuming operation. Besides, the influence of the label on the DNA recognition, varying yields of target−label coupling cannot be excluded.[17] To pass over the needs of target labeling, indirect labeling assays were reported by using a labeled reporter probe, binding to the target overhang at the prehybridized probe−target complex.[18−20] In addition to the easier target preparation, the second hybridization step leads to a higher selectivity; however, a second hybridization step extends the analysis time and is therefore not advantageous for biosensorial point of care use.

Thus, a label-free detection system is preferred, enabling a cost-effective and fast applicability. Here, the hybridization signal is triggered when a complementary target molecule binds to the immobilized probe, resulting in changes of the electrochemical properties of the electrode surface such as conductance, resistance, or surface potential.[16,21−27] This makes the use of a label for impedance analysis unnecessary, whereby also label-based impedance approaches are reported for

Received: May 14, 2014
Accepted: July 6, 2014
Published: July 6, 2014

sensitivity and selectivity enhancement.[28] The large number of published studies using impedance detection for binding analysis show the distinct interest in using this technique for the construction of label-free electrochemical sensors.[5,29−33] This is also attributed to the possibilities of spectra recording over a wide frequency range, allowing for a complete surface characterization in a rather short time. Furthermore, by measuring of just one frequency, real-time measurements of target−probe binding have been shown to be feasible.[34] This gives access to the determination of affinity constants in a similar way to that for optical methods such as surface plasmon resonance spectroscopy.

Previous major efforts in combining impedance spectroscopy and DNA detection focused on sensor sensitivity by changing DNA immobilization methods,[35−37] determining the influence of probe type[38,39] and surface coverage,[40,41] as well as the utilization of different surface materials.[30,42−44] Further approaches showed the potential of impedance spectroscopy to detect single base mismatches,[30,38] but also DNA−protein interactions have been followed by impedance spectroscopy.[41,42,45,46] However, in most cases, rather short targets were used, which are well suited for proof of principle considerations, but the performance of longer strands as, e.g., from PCR amplification protocols have been paid very little attention. There are some other problems in applying EIS for bioanalysis, for example impedance changes with time[45] or lack of reusability.[28] Furthermore, different magnitudes of impedance changes upon hybridization have been reported.[30,47] Thus, more research is needed to obtain well-defined interfaces and detection cycles. This is particularly important for a sensor format, which avoids the detection of labeled molecules.

Thus, in this study, we want to clarify the influence of target length and sequence recognition position on the impedance signal. As a first step, conditions have been evaluated to obtain a sensor system with sufficient signal stability and a reusable application. The sensor consists of a short thiol-modified probe with 25 nucleotides, which is attached to a gold surface and a short mercaptoalcanol to prevent unspecific interactions. As targets, we use differently sized sequences between 25 and 80 nucleotides with varying overhang length and orientation, enabling evaluation of the influence of the respective probe−target complexes on the surface impedance.

MATERIALS AND METHODS

Reagents and Materials. Thiol-modified single-stranded probe oligonucleotides (capture probe) and the complementary oligonucleotides were synthesized by biomers.net (Ulm, Germany). The thiol group was introduced at the 5′-end using a C6-spacer. The DNA concentration was confirmed photometrically, and the content of the free thiol groups was checked using Ellman's reagent.[48] For surface control, a redox-marker, methylene blue (MB), was covalently bound to the amino-C6-modified 5′-end of the complementary ssDNA by biomers.net (Ulm, Germany). All DNA strands have been purified by HPLC. The used ssDNA sequences are listed in Table 1. All other reagents were purchased from Sigma-Aldrich (Taufkirchen, Germany) and were used without additional purification. All solutions were prepared with ultrapure water ("Ultra clear direct" from SG Water, Germany).

For electrochemical investigations, gold chip electrodes have been utilized, which consist of a 200-nm-thick gold film deposited on the silicon chips (10 mm × 20 mm) modified with a titanium and platinum layer as an adhesion promoter. The

Table 1. Sequences of Single-Stranded DNA (ssDNA) Used in This Work[a]

type	oligonucleotide	sequence (5′ → 3′-end)
probe	25mer probe	SH-C_6- CGT CCA AGC GGG CTG ACT CAT CAA G
target	25merMB	MB-C_6-**CTT GAT GAG TCA GCC CGC TTG GAC G**
target	25mer	**CTT GAT GAG TCA GCC CGC TTG GAC G**
target	35mer	TAC AGT ACA C**CT TGA TGA GTC AGC CCG CTT GGA CG**
target	45mer	CCA CTA GCA TTA CAG TAC AC**C TTG ATG AGT CAG CCC GCT TGG ACG**
target	45mer(eo:5)	AGC ATT ACA GTA CAC **CTT GAT GAG TCA GCC CGC TTG GAC G**CC ACT
target	45mer(eo:10)	TAC AGT ACA C**CT TGA TGA GTC AGC CCG CTT GGA CG**C CAC TCC CAT
target	80mer	CAC AAC GCA CTA GGA TGT TCA CAA TCG CAG TCA GAC CAC TAG CAT TAC AGT ACA C**CT TGA TGA GTC AGC CCG CTT GGA CG**
reporter	20mer	GTG TAC TGT AAT GCT AGT GG

[a]Complementary sequence position of the target ssDNA with respect to the 25mer probe or the 20mer reporter are typed in bold and underlined, respectively. SH, thiol; MB, methylene blue; eo, sequence with an overhang exposed to the electrode.

electrodes possess a sensing area of 5 mm in diameter with an area of 0.2 cm^2. QCM-D experiments were performed with gold-coated QSX301 QCM-D chips (4.95 Hz), and SPR experiments were performed with gold coated SPR chips from Biacore (GE Healthcare).

DNA Immobilization. Gold chip electrode, QCM, and SPR chip cleaning was carried out by incubation in "hot piranha" solution (2:1; concentrated sulfuric acid, 98%; hydrogen peroxide solution, 30%) five times for 12 min. Afterward, the electrodes were rinsed thoroughly with deionized water. The freshly cleaned electrodes were modified with thiolized ssDNA (25mer probe) by chemisorption to create a recognition layer. For gold chip electrodes, this was realized by incubating the electrodes in an immobilization buffer (0.1 M potassium phosphate, 1 M potassium chloride, 2 mM magnesium chloride, pH 7) containing 1 μM thiol-modified ssDNA (25mer probe) and 0.5 μM 4-mercapto-1-butanol or 6-mercapto-1-hexanol for 2 h. To remove nonspecifically bound ssDNA and passivate the sensor surface, the electrode incubation was investigated in three different passivation solutions overnight: (1) 1 mM 4-mercapto-1-butanol + immobilization buffer, (2) 1 mM 4-mercapto-1-butanol + measuring buffer (0.1 M sodium phosphate buffer, pH 7), or (3) 1 mM 6-mercapto-1-hexanol + measuring buffer. In contrast, the immobilization on the QCM and SPR chip was performed in a flow system with a flow rate of 5.77 μL/min and 2 μL/min under identical solution and time conditions as described for the gold chip electrodes.

Hybridization and Denaturation. For the electrochemical measurements, hybridization and denaturation were performed in an electrochemical cell. For the hybridization, the modified sensor electrode was incubated for 10 min in stirred 50 mM tris(hydroxymethyl) aminomethane buffer (TRIS/HCl, pH 7) with 100 mM sodium chloride containing 10 μM MB-labeled or unlabeled target ssDNA. For investigations of the sensitivity, concentrations between 0.01 μM and 10 μM were used. After hybridization, the electrode was rinsed five times with measuring buffer to remove unhybridized target ssDNA. To exclude an influence of the measuring sequence, the electrodes

dx.doi.org/10.1021/ac501800q | Anal. Chem. 2014, 86, 7867−7874

were incubated with the corresponding target molecules in a varying order. The denaturation of the hybridized electrode surface was investigated with urea (20 min incubation) and different approaches with deionized water, i.e., 10 min incubation, 10 times rinsing for 3 s, and 10 times rinsing for 3 s followed by an incubation in stirred water for 4 min. Finally, the optimized denaturation protocol with water (10 times rinsing followed by incubation in stirred deionized water for 4 min) was used for further experiments.

For QCM and SPR experiments, the hybridization was performed in a flow system with a flow rate of 50 μL/min and 30 μL/min, respectively, under identical solution and time conditions as described for the electrochemical approach. After each hybridization, the surface was denatured by flushing the QCM and SPR chip with deionized water.

Electrochemical Measurements. All electrochemical measurements were performed with a CHI 604E potentiostat (CH Instruments, Austin, Texas), connected to an electrochemical cell containing the modified gold chip working electrode, an Ag/AgCl, 1 M KCl, reference electrode, and a platinum wire as an auxiliary electrode. For the evaluation of the electrode preparation and to control the amount of hybridizable ssDNA probe, a voltammetric detection method was used.[14] After hybridization of methylene blue-labeled target ssDNA, voltammetric measurements were performed in a measuring buffer. Thereby, the potential was cycled between −0.4 and 0 V at a scan rate of 100 mV/s. By integrating the charge passed when the film is reduced, the total surface coverage of MB-labeled ssDNA can be determined, which is directly related to the surface concentration of hybridizable probes. Subsequently, the surface was regenerated via the established denaturation procedure.

Electrochemical impedance spectroscopy measurements have been carried out in a measuring buffer containing 2 mM ferri- and ferrocyanide (each) with the following parameters: 10 kHz−1 Hz frequency range, 5 mV AC amplitude, and open circuit potential (OCP). Before each impedimetric measurement, the OCP (180−190 mV vs Ag/AgCl) was determined and applied to the working electrode. The obtained impedance spectra were analyzed by use of an equivalent circuit, which consists of a parallel circuit containing a charge transfer resistance (R_{ct}) and a constant phase element (CPE) as well as a solution resistance (R_{sol}) in series. The α value of the CPE was between 0.95 and 0.97, allowing evaluation of the capacitive behavior of the interfaces.

QCM Measurements. For real-time measurements of the immobilization and hybridization, we used a qsense E4 QCM-D from Biolin Scientific, which measures simultaneously the frequency (Δf) and dissipation change (ΔD). The third overtone was used for the analysis of the experiments. Experimental conditions are described under immobilization as well as hybridization and denaturation.

SPR Measurements. SPR measurements were performed during immobilization and hybridization with a Biacore T100, determining the SPR angle shift ($\Delta\theta$). The SPR signal was converted to the attached mass according to the device manufacturer's instructions (1000 RU = 100 ng/cm^2). Experimental conditions are described under immobilization as well as hybridization and denaturation.

RESULTS AND DISCUSSION

Sensor Principle and Characterization. For the preparation of the sensor, a short thiol-modified probe ssDNA, serving as a recognition element, is attached to the gold chip electrodes. We choose probe ssDNA with a length of 25 nucleotides, which usually provides higher hybridization specificity and efficiency compared to longer ssDNA.[4] Additionally, 4-mercapto-1-butanol (MCB) is used to remove unspecific ssDNA interactions on the gold surface and promote the orientation of the probe ssDNA to the solution but also to enable a high flexibility of the probe.[14]

To evaluate the quality of the prepared ssDNA electrodes, the chip is characterized with respect to the amount of hybridizable probe ssDNA by using a hybridization step with a methylene blue modified target ssDNA (25merMB) followed by voltammetric analysis.[14] The surface coverage of functional probe ssDNA is determined from the reduction peak area that corresponds to the bound 25merMB. Since different studies demonstrate the influence of probe density on the hybridization efficiency and sensor performance,[40,41,49] we have used electrodes with a rather similar surface coverage (11.5 ± 2.2 pmol/cm^2, n = 32) to ensure good reproducibility and comparability of the experiments.

Subsequently, the electrodes are investigated before and after hybridization with 25mer target ssDNA in the presence of the redox system (ferri-/ferrocyanide) by impedance spectroscopy. The obtained impedance spectra represent the electrochemical interaction between the redox system and the DNA-modified electrode. To ensure a fast sensorial applicability, the hybridization is reduced to a very short time of just 10 min. The impedance spectra of an electrode with a denatured and hybridized surface are illustrated in Figure 1. Here, the

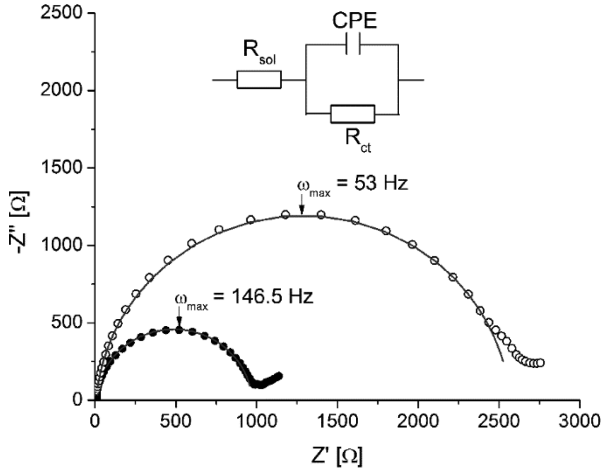

Figure 1. Impedance spectra of a denatured (solid symbols) and hybridized (open symbols) sensor surface depicted as a Nyquist plot. Inset: Equivalent circuit that is used for the analysis of the obtained data in this work (R_{sol}, solution resistance; R_{ct}, charge transfer resistance; CPE, constant phase element representing the double layer capacity). The resulting fit is plotted as a solid line. ω_{max} is evaluated from the fit curve.

semicircle diameter correlates with the charge transfer resistance and enables a first estimation resulting in an approximately 2.5 times higher resistance after hybridization. These observations can be attributed to a further accumulation of negative charges as a result of the target binding, which disturbs the conversion of the negatively charged redox system at the electrode. The recorded impedance spectra have been analyzed by an equivalent circuit (Figure 1 inset) consisting of a solution resistance (R_{sol}), a charge transfer resistance (R_{ct}), and a

dx.doi.org/10.1021/ac501800q | Anal. Chem. 2014, 86, 7867−7874

constant phase element (CPE), which possesses an α value of 0.95−0.97 and, thus, is almost equal to the double layer capacity (C_{dl}). Since the frequency range influenced by diffusion has been excluded from the analysis, an integration of the Warburg impedance can be avoided. After hybridization with 25mer target ssDNA, the charge transfer resistance increases from 700 ± 230 Ω to 1990 ± 580 Ω (n = 8) and allows good discrimination between the denatured and hybridized situation. Despite the differences of each electrode with respect to the absolute charge transfer resistance, the R_{ct} ratio among the denatured and hybridized situation is quite similar (2.6 ± 0.17) and has been chosen as the sensor parameter for the DNA detection. In contrast, the hybridization induces only a slight increase of the capacity of 8%.

Sensor Regeneration. The denaturation is an essential step to regenerate the sensor after hybridization and ensures a reuseability for a sustainable and economical operation. Therefore, we have tested different denaturation reagents and strategies with methylene blue labeled targets by means of voltammetry. First, urea is used which has been shown to perform well with shorter strands.[30] However, it is found that denaturation does not fully complete. Thus, we have searched for an alternative, more efficient denaturation procedure. Deionized water is subsequently tested with respect to its ability to separate DNA strands. The denaturation principle of deionized water is based on the destabilization of the duplex due to the lack of shielding of negative DNA charges in the absence of cations, inducing an electrostatic repulsion of the individual strands. Three different denaturation methods with deionized water are investigated, i.e., 10 min incubation, 10 times rinsing of the chip for 3 s, and 10 times rinsing of the chip for 3 s followed by an incubation under stirring for 4 min (Figure 2).

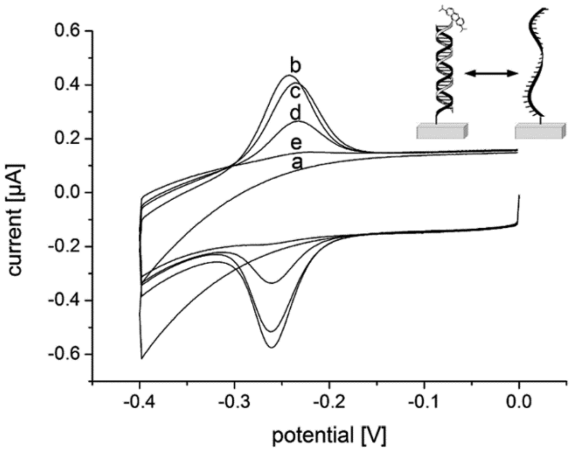

Figure 2. Cyclic voltammograms of an electrode before (a) and after hybridization (b) with complementary methylene blue modified target ssDNA (25merMB) as well as after application of different denaturation procedures with deionized water: 10 min incubation (c), 10 × rinse for 3 s (d), 10 × rinse for 3 s and 4 min incubation under stirring (e).

While the incubation in water for 10 min results only in a weak removal of 25merMB ssDNA (14%), the denaturation efficiency increases up to 60% by rinsing with water and can be enhanced to nearly 100% by additionally stirring for 4 min. This means that, by adjustment of suitable convective conditions, an efficient denaturation procedure with water can be established. By using this procedure, four repeated hybridization/denaturation cycles are performed while maintaining the same hybridization and denaturation efficiency (with an average of 98.5 ± 2% for hybridization and 97 ± 1% for denaturetion) for each cycle without noticing electrode aging. Thus, the electrode functionality is not affected by the denaturation procedure, and a consistent quality of voltammetric DNA detection during the cycles is feasible.

Signal Stability and Sensitivity. Although the DNA electrodes have been found reusable, impedance changes for repeated hybridization/denaturation cycles have been observed.[30] Such problems have also been mentioned sometimes in the literature.[50,51]

The new denaturation procedure described in this study results in a rather complete removal of the bound target strand; thus the impedimetric signal stability for repeated measurements is investigated. Figure 3A shows impedance spectra of a DNA electrode for three repetitive cycles of denaturation and hybridization with 25mer target ssDNA. A clear increase of the charge transfer resistance during the measuring procedure is determined, indicating a change of the electrode surface properties. Since the impedance signal increase also occurs without target strands, the DNA electrode is probably subjected to a time-dependent chip aging, which has also been found with urea as denaturation agent. Additionally, the impedimetric signal instability results in a slight decrease of the R_{ct} ratio between the hybridized and denatured situation of the corresponding cycle (first cycle 2.48; second cycle 2.31; third cycle 2.27). This means that in contrast to the voltammetric studies a signal loss during the detection cycles is observed with the impedimetric system despite the same working conditions. Although this effect is not large, it limits the applicability of the sensor system. Consequently, we have tried to improve the stability of the sensing surface.

First, we consider the ionic composition of the buffers used during sensor preparation, since the solution properties are found to possess an important influence on the interfacial impedance of DNA layers.[17] Therefore, we exchange the high-molar immobilization buffer (0.1 M potassium phosphate, 1 M potassium chloride, 2 mM magnesium chloride) during the passivation with MCB by measuring buffer (0.1 M sodium phosphate) with a clearly smaller ionic strength to avoid a DNA rearrangement at the electrode after buffer changes. Here, a first improvement of the impedance stability is observed, resulting in a smaller impedance increase: 50% of the denatured situation of the first and third cycle compared to 142% for the electrodes prepared in immobilization buffer.

On the basis of these results, we examine the influence of the passivation reagent by using 6-mercapto-1-hexanol (MCH) rather than 4-mercapto-1-butanol during the sensor preparation. As illustrated in Figure 3B, the MCH/DNA electrode is denatured and hybridized three times and shows good reproducibility of DNA detection without time dependent impedance changes. Furthermore, by using MCH and avoiding buffer changes, the R_{ct} ratio for the denatured and hybridized electrodes remains at 2.73 ± 0.25 (n = 8), although absolute R_{ct} values are around 1 order of magnitude higher compared to DNA electrodes with MCB. The latter observation is a clear argument for a better isolation of the MCH/DNA electrodes for the redox couple ferri-/ferrocyanide. Thus, the improved impedance signal stability can be attributed to the longer chain length of MCH, enabling a more ordered monolayer on the DNA electrode and diminishing nonspecific DNA−gold interactions. This can be also beneficial for the protection of the

dx.doi.org/10.1021/ac501800q | Anal. Chem. 2014, 86, 7867−7874

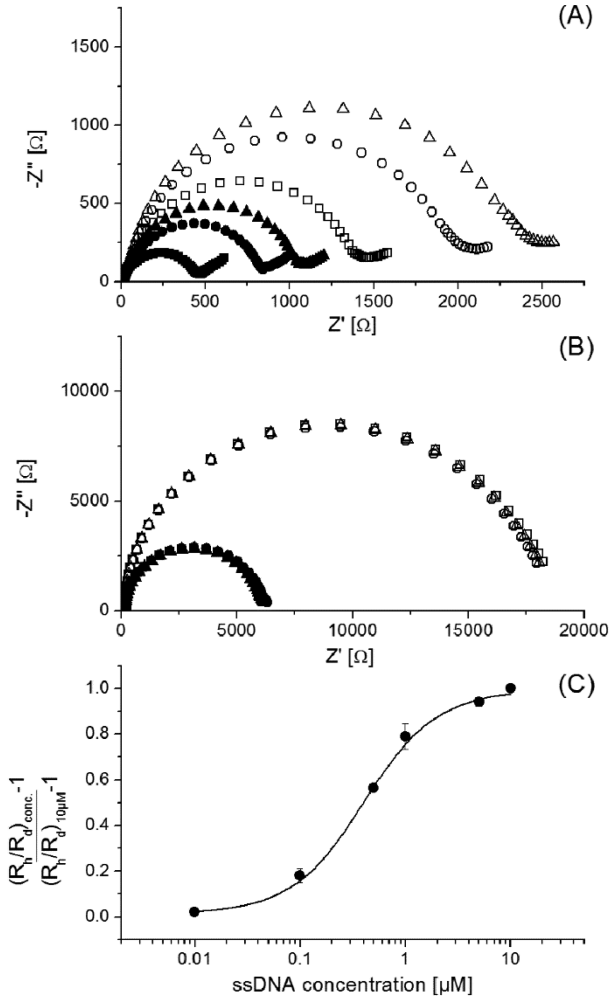

Figure 3. Impedance spectra of an ssDNA electrode prepared with MCB (A) and MCH (B) after three cycles of denaturation (solid symbols) and hybridization (open symbols) with 25mer target ssDNA (first cycle, squares; second cycle, circle; third cycle, triangle). (C) Relative ratio of charge transfer resistance of ssDNA electrodes (n = 3) prepared with MCH depending on the 25mer target ssDNA concentration. The data are normalized to the value obtained for 10 μM 25mer target ssDNA: (R_h/R_d)conc., charge transfer resistance ratio between the hybridized (h) and denatured (d) situation after incubation with different concentrations of 25mer target ssDNA; $(R_h/R_d)10$ μM, charge transfer resistance ratio between the hybridized (h) and denatured (d) situation after incubation with 10 μM 25mer target ssDNA.

electrode surface against unspecific interactions with the analyte or other interfering molecules. Although MCB seems to be well suited as a protective layer in a voltammetric analysis of DNA hybridization, it provides not enough stability as a layer for a reusable impedimetric sensor. In conclusion, it can be stated that by avoiding complete buffer changes during sensor preparation, applying a longer thiol as passivating agent and using a rather soft method for DNA denaturation conditions have been found to improve the stability of the system allowing sensorial DNA detection.

Consequently, MCH/DNA electrodes are investigated with different concentrations of 25mer ssDNA to determine the detection limit and the dynamic range. The results of the impedimetric analysis are depicted in Figure 3C as the normalized R_{ct} ratio dependent on the ssDNA concentration. We have found a sigmoidal binding curve with increasing R_{ct} after hybridization with concentrations between 0.01 μM and 10 μM 25mer ssDNA. Hence, a half-maximum concentration of 380 ± 50 nM and a linear concentration range between 0.15 μM and 1 μM is determined, which is similar to the concentration range of an impedimetric sensor using shorter target ssDNA[30] and a voltammetric sensor using labeled ssDNA.[14] It should be mentioned here that this sensitivity is reached within a rather short time of hybridization and without application of any enhancement strategy (e.g., field-assisted accumulation near the sensor surface).

Influence of Target Length and Recognition Sequence Position. Although sensitivity in the nanomolar range can be provided, often amplification is necessary for practical detection of small DNA amounts. Here, however, much longer strands occur after PCR and ds denaturation. Thus, we have performed hybridization studies with differently sized complementary targets. All sequences used are designed with a similar small theoretical tendency for the formation of secondary structures in order to minimize structural influences on the hybridization efficiency. First, we have considered sequences with an overhang exposed to the solution after binding to the immobilized probe in the range between 35 and 80 nucleotides length (i.e., 35mer, 45mer, and 80mer ssDNA). The design of the hybridized probe−target complexes is schematically shown in Scheme 1.

Scheme 1. Schematic Illustration of the Probe−Target Complex between a 25mer Probe and the Corresponding Target ssDNA of Different Length

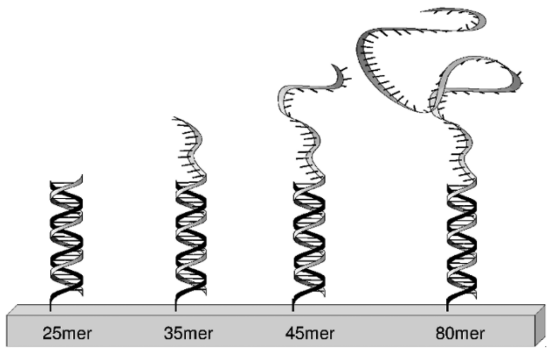

As shown in Figure 4A, for all target sequences an increasing impedance is found after hybridization. However, contrary to our expectations the R_{ct} change decreases with increasing target length, although the binding of longer strands results in a higher mass accumulation, associated with a rise of negative charges in front of the electrode (Figure 4C). This observation is expressed in a decrease of the R_{ct} ratio of the 35mer, 45mer, and 80mer compared to the ratio of the 25mer target ssDNA (see Table 2). Since a decreased hybridization efficiency is known for longer strands,[52] an influence of lower amounts of dsDNA on the impedimetric signal response cannot be excluded. However, the impedimetric experiments do not give insights into the hybridization efficiency or conformational effects of probe−target complexes of the respective targets. Therefore, the hybridization of the differently sized targets is investigated by quartz crystal microbalance (QCM-D) and surface plasmon resonance spectroscopy (SPR). The construction of the DNA/MCH sensing layer at the SPR and QCM chip as well as the hybridization with target ssDNA is performed

dx.doi.org/10.1021/ac501800q | Anal. Chem. 2014, 86, 7867−7874

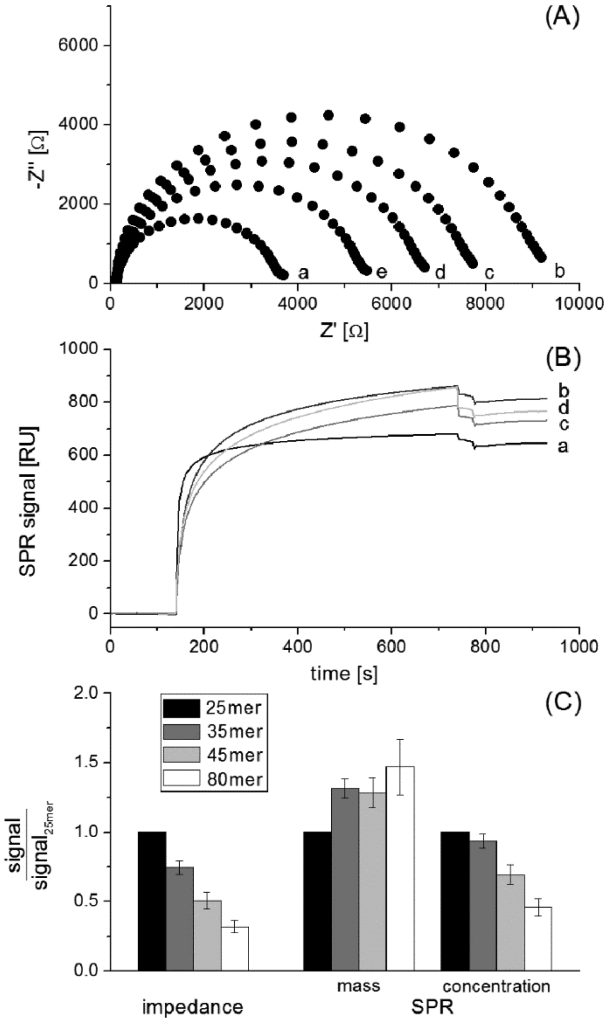

Figure 4. (A) Impedance spectra of an electrode before (a) and after hybridization with 25mer (b), 35mer (c), 45mer (d), and 80mer (e) target ssDNA, respectively. (B) SPR measurements of the hybridization with 25mer (a), 35mer (b), 45mer (c), and 80mer (d) target ssDNA on a 25mer probe/MCH modified SPR chip. (C) Normalized hybridization signal of the impedance and SPR experiments for the hybridization with 25mer, 35mer, 45mer, and 80mer target ssDNA. The impedimetric signal is determined by the charge transfer resistance ratio $[(R_h/R_d) - 1]$ between the hybridized and denatured situation. The mass and concentration of the bound targets are calculated from the SPR signal.

in a flow system, but under the same conditions as used for the impedimetric sensor.

Although other studies show that the use of QCM is inappropriate for the quantitative determination of bound ssDNA,[53] because of the additional detection of the hydration shell (bound water), the dissipation is found to be directly related to the intrinsic viscosity, providing information about the hydrodynamic size and shape of molecules.[54] From the QCM-D measurements, we obtain the mass-related frequency shift (Δf) and the viscosity-sensitive dissipation change (ΔD) after the hybridization of the 25mer, 35mer, 45mer, and the 80mer target ssDNA (see Table 2). Here, the extension of the target strands increases both Δf and ΔD. Interestingly, we have observed a different dissipative behavior between the hybridized 25mer targets and hybridized probe−target complexes with an overhang. While the binding of 25mer targets results in a negative dissipation, which is attributed to the formation of a DNA layer with an increasing stiffness, an additional overhang increases the dissipation with increasing length. This means that the single-stranded overhangs increase the electrode surface viscosity and dominate over the stiff duplex areas. The QCM-D experiments verify the different situation on the electrode surface after hybridization of the respective targets and may give a first hint for the various impedance signals after binding of targets with different lengths.

Subsequently, SPR measurements have been performed in order to determine the hybridization efficiencies of the differently sized ssDNA targets (as shown in Figure 4B). We find for the 25mer target ssDNA a stable SPR signal at the end of 10 min of incubation, indicating the formation of a completely hybridized chip surface. In contrast, the targets with overhang show a still increasing SPR signal at the termination of the hybridization, giving a clear hint for slower hybridization kinetics of longer strands. For the analysis, the attached mass of the bound targets is determined from the SPR signal response (1000 RU = 100 ng/cm^2) in order to calculate the surface concentration of probe−target complexes (see Table 2). We find that an increase of the target length results in an increase of attached (hybridized) mass, whereby the molar surface concentration of probe−target complexes decreases by the use of longer sequences. Thus, a reduction of hybridization efficiency for longer targets can be obtained that reflects the steric and repulsive hindrance of the overhanging extensions of the long targets and is in good agreement with other reports.[52,55] With respect to the impedimetric experiments, this means that the R_{ct} change follows the surface concentration of formed target−probe complexes (Figure 4C). It can be concluded that a high surface density of probe−target complexes is more important than the finally attached DNA mass, when a large part of the DNA is located away from the

Table 2. Experimental Results of Hybridization Studies of Different Targets to the 25mer Probe after 10 min from EIS, SPR, and QCM-D Experiments

	EIS[a]	SPR[b]		QCM-D	
oligomer	R_h/R_d	mass [ng/cm^2]	concentration [pmol/cm^2]	Δf [Hz]	dissipation (10^{-6})
25mer	2.4 ± 0.11	56.2 ± 7.3	7.3 ± 0.9	9.7 ± 0.9	−0.32 ± 0.12
35mer	2.06 ± 0.12	71.3 ± 7.9	6.6 ± 0.7	17.9 ± 0.4	0.64 ± 0.21
45mer	1.72 ± 0.13	68.7 ± 5.3	5 ± 0.4	20.2 ± 0.9	1.73 ± 0.15
80mer	1.46 ± 0.08	79.1 ± 4.3	3.2 ± 0.2	22.7 ± 1.2	3.26 ± 0.22
45mer(eo:5)	2.03 ± 0.08	69.9 ± 5.5	5.1 ± 0.4		
45mer(eo:10)	2.25 ± 0.07	64.2 ± 5.3	4.7 ± 0.4		

[a]Ratio of charge transfer resistance (R_h/R_d) between hybridized and denatured sensor surface. [b]Mass and concentration calculated from SPR signal according to the device manufactures instructions (1000 RU = 100 ng/cm^2).

dx.doi.org/10.1021/ac501800q | Anal. Chem. 2014, 86, 7867−7874

electrode. Consequently, the accumulation of negative charges due to the overhang possesses less influence on the impedance signal than expected. We suggest that DNA positioned near the electrode surface increases the electrostatic repulsion between the electrode surface and ferri-/ferrocyanide anions in a stronger way and is more difficult to permeate for the complex ion.

However, the sensor clearly demonstrates the potential for the detection of longer ssDNA up to a length of 80 nucleotides after a short hybridization time of just 10 min, which is beneficial for the detection of PCR products.

On the basis of these experiments, we have tested whether a second hybridization with a 20mer ssDNA that is complementary to a region of the captured 45mer or 80mer target ssDNA next to the probe can be used as a further enhancement step (see Table 1). This means that after the second hybridization step the double-stranded part of the probe–target complex is extended from 25 base pairs to 45 base pairs and induces a further accumulation of negative charges in front of the electrode in addition to the conformational change of the overhang. SPR experiments clearly show a successful binding at the overhang of both the 45mer and 80mer with a calculated hybridization efficiency of around 69% (with the surface concentration of the 45mer and 80mer, respectively, taken as 100%). However, by use of the impedimetric sensor, only a slight R_{ct} change is observed after hybridization of the 20mer at the overhang of the 45mer as well as the 80mer target ssDNA (data not shown). Thus, the increase of negative charge in a larger distance from the electrode surface does not contribute crucially to the signaling process.

We finally examine how the impedimetric signal can be enhanced for longer strands in a different way: Thus, we have changed the position of the recognition sequence within the target strands. We use a 45mer(eo:5) and 45mer(eo:10), which possess a 5 and 10 nucleotide long overhang exposed to the electrode surface. Due to the orientation of the overhang near the electrode, a further accumulation of negative charge and an increase of the R_{ct} compared to the 45mer can be expected. However, due to the overhang, steric and repulsive effects can occur that may influence the hybridization kinetics of the respective target. Unfortunately, previous studies are controversial in terminating the effect of overhang exposition on the hybridization efficiency,[8,52,55] which is probably caused by different hybridization conditions such as probe immobilization chemistry, probe surface coverage, and probe length. Figure 5 illustrates representative impedimetric spectra of an electrode before and after hybridization with various 45mer ssDNA targets. Despite different recognition sequence positions, all investigated 45mer molecules trigger an impedance change after the respective hybridization event and are detectable. However, there is a clear difference of impedance behavior between the probe–target complex, which possess an overhang of 20 nucleotides exposed to the solution, and the complexes in which the target is partly exposed to the electrode surface, i.e., 45mer(eo:5) and 45mer(eo:10). The obtained R_{ct} ratio increases for the 45mer, 45mer(eo:5), and 45mer(eo:10) from 1.72 ± 0.13 to 2.03 ± 0.08 and 2.25 ± 0.07, respectively, and shows a dependence between the R_{ct} change and the length of the overhang exposed to the electrode surface. In order to exclude concentration-related effects on the impedimetric signal, SPR investigations are performed, observing only a slightly decreased surface concentration of the formed dsDNA with an increasing length of overhang exposed to the electrode

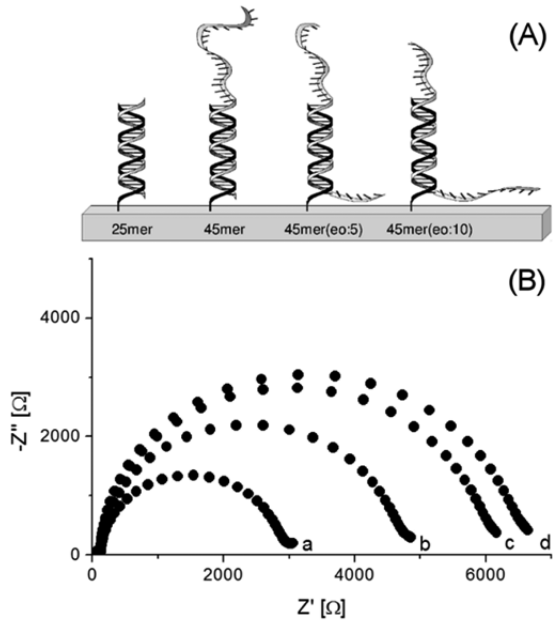

Figure 5. (A) Schematic illustration of the probe–target complexes between a 25mer probe and the different target ssDNA. (B) Impedance spectra of an electrode before (a) and after hybridization with 45mer (b), 45mer(eo:5) (c), and 45mer(eo:10) (d) target ssDNA, respectively (eo:5 and eo:10 mean that 5 or 10 nucleotide overhangs are exposed to the electrode side).

(see Table 2). The low effect of steric hindrance can be explained by the medium surface concentration of hybridizable probe DNA on the electrode used in this study. The impedimetric effect of the bottom overhang can be clearly contributed to the direct increase of negative charges near the electrode, which disturbs the permeation of ferri-/ferrocyanide to the electrode. The results suggest that the impedimetric system enables the distinction of targets with the same size, but a different sequence recognition position. Furthermore, this gives access to the design of beneficial probe–target complexes, resulting in an enhanced impedimetric signal response, and may allow the label-free detection of targets even longer than the presented 80mer.

■ CONCLUSIONS

To conclude, we have investigated an impedimetric sensor for the label-free detection of nucleic acids, which gives access to a fast and less imperious analysis. Our results demonstrate that the choice of buffer during the sensor preparation and the passivation reagent possess a crucial influence on the signal stability of the interfacial impedance. Here, the use of a mercaptoalcanol with a longer chain length leads to a formation of a more stable layer, ensuring a stable impedance signal in repeated hybridization/denaturation cycles. Furthermore, we developed an effective and gentle regeneration protocol that enables a reusability of the sensor without observing aging effects of the electrode. Both the stable impedance signal and the regeneration protocol allow the determination of different concentrations of complementary 25mer with a detection limit in the low nanomolar range but also the investigation of the target length and recognition sequence position influence on the impedimetric behavior. We find a relation between the target length of sequences with overhangs exposed to the solution and the charge transfer resistance change, which is on

dx.doi.org/10.1021/ac501800q | Anal. Chem. 2014, 86, 7867–7874

the one hand attributed to the lower hybridization efficiency of longer targets but also due to the lower impact of the ssDNA overhangs far away from the electrode on the sensorial signal response. We can demonstrate the label-free impedimetric detection of target strands up to 80 nucleotides length by applying only a short hybridization time of 10 min, which gives access to a detection of PCR products from biochemical samples. An additional amplification step by a second hybridization at the overhang of the probe−target complex results only in minor impedance changes. Alternatively, we show that the charge transfer resistance is increasing by changing the recognition sequence position in equally sized target strands, i.e., shifting the overhang position from solution to the electrode surface. In summary, one can state that some obstacles in using electrochemical impedance spectroscopy for DNA detection have been overcome.

AUTHOR INFORMATION

Corresponding Author

*E-mail: flisdat@th-wildau.de.

Notes

The authors declare no competing financial interest.

ACKNOWLEDGMENTS

The authors thank H. Iken for technical support in preparing the gold chip electrodes.

REFERENCES

(1) Mikkelsen, S. R. *Electroanalysis* **1995**, *8*, 15−19.
(2) Drummond, T. G.; Hill, M. G.; Barton, J. K. *Nat. Biotechnol.* **2003**, *21*, 1192−1199.
(3) Wang, J. *Biosens. Bioelectron.* **2006**, *21*, 1887−1892.
(4) Lucarelli, F.; Tombelli, S.; Minunni, M.; Marrazza, G.; Mascini, M. *Anal. Chim. Acta* **2008**, *609*, 139−159.
(5) Lisdat, F.; Schäfer, D. *Anal. Bioanal. Chem.* **2008**, *391*, 1555−1567.
(6) Sassolas, A.; Leca-Bouvier, B. D.; Blum, L. J. *Chem. Rev.* **2008**, *108*, 109−139.
(7) Wu, V. C. H.; Chen, S.; Lin, C. *Biosens. Bioelectron.* **2007**, *22*, 2967−2975.
(8) Kleo, K.; Kapp, A.; Ascher, L.; Lisdat, F. *Anal. Biochem.* **2011**, *418*, 260−266.
(9) Pollet, J.; Delport, F.; Janssen, K. P. F.; Jans, K.; Maes, G.; Pfeiffer, H.; Wevers, M.; Lammertyn, J. *Biosens. Bioelectron.* **2009**, *25*, 864−869.
(10) Fan, X.; White, I. M.; Shopova, S. I.; Zhu, H.; Suter, J. D.; Sun, Y. *Anal. Chim. Acta* **2008**, *620*, 8−26.
(11) Nöll, G.; Su, Q.; Heidel, B.; Yu, Y. *Adv. Healthcare Mater.* **2014**, *3*, 42−46.
(12) Palecek, E.; Bartosik, M. *Chem. Rev.* **2012**, *112*, 3427−3481.
(13) Akhavan, O.; Ghaderi, E.; Rahighi, R. *ACS Nano* **2012**, *6*, 2904−2916.
(14) Pänke, O.; Kirbs, A.; Lisdat, F. *Biosens. Bioelectron.* **2007**, *22*, 2656−2662.
(15) Aoki, H.; Tao, H. *Analyst* **2007**, *132*, 784−791.
(16) Poghossian, A.; Cherstvy, A.; Ingebrandt, S.; Offenhäuser, A.; Schöning, M. J. *Sens. Actuators, B* **2005**, *111−112*, 470−480.
(17) Daniels, J. S.; Pourmand, N. *Electroanalysis* **2007**, *19*, 1239−1257.
(18) Zhao, X.; Tapec-Dytioco, R.; Tan, W. *J. Am. Chem. Soc.* **2003**, 11474−11475.
(19) Umek, R. M.; Lin, S. W.; Vielmetter, J.; Terbrueggen, R. H.; Irvine, B.; Yu, C. J.; Kayyem, J. F.; Yowanto, H.; Blackburn, G. F.; Farkas, D. H.; Chen, Y. P. *J. Mol. Diagn.* **2001**, *3*, 74−82.
(20) Campbell, C. N.; Gal, D.; Cristler, N.; Banditrat, C.; Heller, A. *Anal. Chem.* **2002**, *74*, 158−162.
(21) Berggren, C.; Stalhandske, P.; Brundell, J.; Johansson, G. *Electroanalysis* **1999**, *11*, 156−160.
(22) Pan, S.; Rothberg, L. *Langmuir* **2005**, *21*, 1022−1027.
(23) Wang, J.; Jiang, M.; Fortes, A.; Mukherjee, B. *Anal. Chim. Acta* **1999**, *402*, 7−12.
(24) Li, C. Z.; Liu, Y.; Luong, J. H. *Anal. Chem.* **2005**, *77*, 478−485.
(25) Star, A.; Tu, E.; Niemann, J.; Gabriel, J. P.; Joiner, C. S.; Valcke, C. *Proc. Natl. Acad. Sci. U.S.A.* **2006**, *103*, 921−926.
(26) Ingebrandt, S.; Han, Y.; Nakamura, F.; Poghossian, A.; Schöning, M. J.; Offenhäuser, A. *Biosens. Bioelectron.* **2007**, *22*, 2834−2840.
(27) Uno, T.; Tabata, H.; Kawai, T. *Anal. Chem.* **2007**, *79*, 52−59.
(28) Patolsky, F.; Katz, E.; Bardea, A.; Willner, I. *Langmuir* **1999**, *15*, 3703−3706.
(29) Park, J. Y.; Park, S. M. *Sensors* **2009**, *9*, 9513−9532.
(30) Kafka, J.; Pänke, O.; Abendroth, F.; Lisdat, F. *Electrochim. Acta* **2008**, *53*, 7467−7474.
(31) Long, Y. T.; Li, C. Z.; Kraatz, H.; Lee, J. S. *Biophys. J.* **2003**, *84*, 3218−3225.
(32) Gebala, M.; Schuhmann, W. *ChemPhysChem* **2010**, *11*, 2887−2895.
(33) Corrigan, D. K.; Schulze, H.; Henihan, G.; Ciani, I.; Giraud, G.; Terry, J. G.; Walton, A. J.; Pethig, R.; Ghazal, P.; Crain, J.; Campbell, C. J.; Mount, A. R.; Bachmann, T. T. *Biosens. Bioelectron.* **2012**, *34*, 178−184.
(34) Vermeeren, V.; Bijnens, N.; Wenmackers, S.; Daenen, M.; Haenen, K.; Williams, O. A.; Ameloot, M.; vandeVen, M.; Wagner, P.; Michiels, L. *Langmuir* **2007**, *23*, 13192−13202.
(35) Park, J. Y.; Kwon, S. H.; Park, J. W.; Park, S. M. *Anal. Chim. Acta* **2008**, *619*, 37−42.
(36) Lee, T. Y.; Shim, Y. B. *Anal. Chem.* **2001**, *73*, 5629−5632.
(37) Peng, H.; Soeller, C.; Travas-Sejdic, J. *Macromolecules* **2007**, *40*, 909−914.
(38) Wang, Y.; Li, C.; Li, X.; Li, Y.; Kraatz, B. *Anal. Chem.* **2008**, *80*, 2255−2260.
(39) Keighley, S. D.; Estrela, P.; Li, P.; Migliorato, P. *Biosens. Bioelectron.* **2008**, *24*, 906−911.
(40) Keighley, S. D.; Li, P.; Estrela, P.; Migliorato, P. *Biosens Bioelectron.* **2008**, *23*, 1292−1297.
(41) Witte, C.; Lisdat, F. *Electroanalysis* **2011**, *23*, 339−346.
(42) Li, X.; Shen, L.; Zhang, D.; Qi, H.; Gao, Q.; Zhang, C. *Biosens. Bioelectron.* **2008**, *23*, 1624−1630.
(43) Chen, C. P.; Ganguly, A.; Wang, C. H.; Hsu, C. W.; Chattopadhyay, S.; Hsu, Y. K.; Chang, Y. C.; Chen, K. H.; Chen, L. C. *Anal. Chem.* **2009**, *81*, 36−42.
(44) Cai, W.; Peck, J. R.; van der Weide, D. W.; Hamers, R. J. *Biosens. Bioelectron.* **2004**, *19*, 1013−1019.
(45) Tersch, C.; Lisdat, F. *Electrochim. Acta* **2011**, *56*, 7673−7679.
(46) Gong, H.; Zhong, T.; Gao, L.; Li, X.; Bi, L.; Kraatz, H. *Anal. Chem.* **2009**, *81*, 8639−8643.
(47) Gebala, M.; Stoica, L.; Neugebauer, S.; Schuhmann, W. *Electroanal.* **2008**, *21*, 325−331.
(48) Riddles, P. W.; Andrews, R. K.; Blakeley, R. L.; Zerner, B. *Biochim. Biophys. Acta* **1983**, *743*, 115.
(49) Peterson, A. W.; Heaton, R. J.; Georgiadis, R. M. *Nucleic Acids Res.* **2001**, *29*, 5163−5168.
(50) Javamard, M.; Esfandyarpour, H.; Pease, F.; Davis, R. W. *J. Vac. Sci. Technol., B: Nanotechnol. Microelectron.: Mater., Process., Meas., Phenom.* **2010**, *27*, 3099−3103.
(51) Bogomolova, A.; Komarova, E.; Reber, K.; Gerasimav, T.; Yavut, O.; Bhatt, S.; Aldissi, M. *Anal. Chem.* **2009**, *81*, 3944−3949.
(52) Baker, B. A.; Milam, V. T. *Nucleic Acids Res.* **2011**, *39*, e99.
(53) Su, X.; Wu, Y. J.; Knoll, W. *Biosens. Bioelectron.* **2005**, *21*, 719−726.
(54) Tsortos, A.; Papadakis, G.; Gizeli, E. *Biosens. Bioelectron.* **2008**, *24*, 836−841.
(55) McKendry, R.; Zhang, J.; Arntz, Y.; Strunz, T.; Hegner, M.; Lang, H. P.; Baller, M. K.; Certa, U.; Meyer, E.; Güntherodt, H.; Gerber, C. *Proc. Natl. Acad. Sci. U.S.A.* **2002**, *99*, 9783−9788.